THE MIXING EFFICIENCY OF OPEN FLOWS

By

Jean-Luc Thiffeault
and
Charles R. Doering

IMA Preprint Series # 2300

(March 2010)

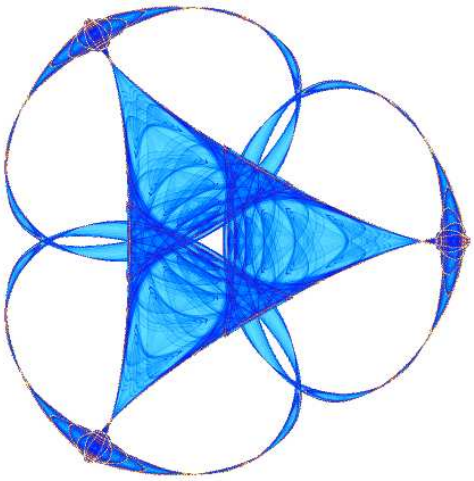

INSTITUTE FOR MATHEMATICS AND ITS APPLICATIONS

UNIVERSITY OF MINNESOTA
400 Lind Hall
207 Church Street S.E.
Minneapolis, Minnesota 55455–0436

Phone: 612-624-6066 Fax: 612-626-7370
URL: http://www.ima.umn.edu

The Mixing Efficiency of Open Flows

Jean-Luc Thiffeault[1,3,*] and Charles R. Doering[2,3,†]

[1]*Department of Mathematics, University of Wisconsin, Madison, WI, USA*
[2]*Departments of Mathematics, Physics, and Center for Study of Complex Systems, University of Michigan, Ann Arbor, MI, USA*
[3]*Institute for Mathematics and Applications, University of Minnesota, Minneapolis, MN, USA*

(Dated: March 3, 2010)

Mixing in open incompressible flows is studied in a model problem with inhomogeneous passive scalar injection on an inlet boundary. As a measure of the efficiency of stirring, the bulk scalar concentration variance is bounded and the bound is shown to be sharp at low Péclet number. Although no specific flow saturating the bound at high Péclet number is produced here, the estimate is conjectured to be approached for flows possessing sufficiently sustained chaotic regions.

I. INTRODUCTION

Since the pioneering work of L. N. Howard [1], applied physicists and mathematicians have found that rigorous bounds are a straightforward way of obtaining useful estimates on fluxes of quantities transported by complex incompressible flows, from laminar to fully developed turbulent flows. In recent years the co-authors and collaborators [2–7] and others [8–12] used similar ideas to bound mixing efficiencies for processes described by the advection-diffusion equation with inhomogeneous passive scalar sources and sinks. One major insight emerging from these studies is the distinction between transient mixing problems, where concentration inhomogeneities are provided by initial conditions, and (statistically) steady mixing in the presence of sustained sources and sinks. In the former case the flow's shearing and straining properties, i.e., the stretching and folding of material lines, serve to enhance the effect of molecular diffusion and increase the rate of scalar concentration variance dissipation. On the other hand, in the latter case the spatial variation of the concentration is best suppressed by direct transport of material from sources to sinks and vice versa. Then the maximum possible enhancement of molecular diffusion by stirring is limited not by small scale features in the flow, but rather by small scale properties of the sources and sinks [3–5].

In this paper we extend these techniques to the case of fluxes at the boundaries rather than body sources as previously described. This is not just a mathematical detail: the problem changes significantly. Notably, the scalar inhomogeneities are transported away from both source and sink regions so the transient mixing efficiency of downstream regions of the stirring flow are crucial for efficient mixing. At the same time the source-sink structure defined by the distribution of fluxes on the boundary plays a key role in the maximum possible mixing efficiency. In the remainder of this paper we define a specific scenario where these issues can be addressed and study it via general analysis and particular examples.

*Electronic address: jeanluc@math.wisc.edu
†Electronic address: doering@umich.edu

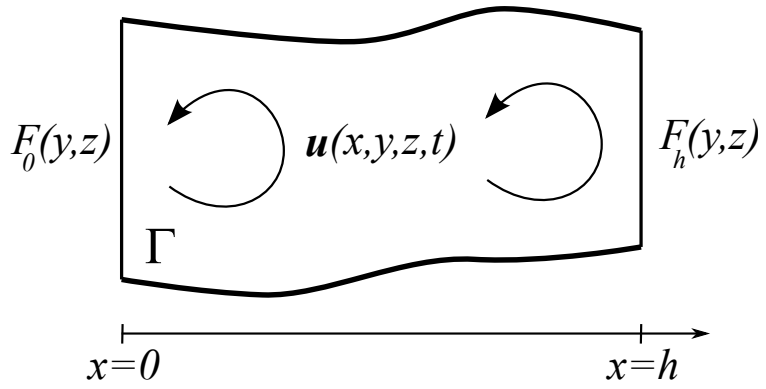

FIG. 1: Schematic of the flow domain Γ. The scalar flux is imposed at $x = 0$ and $x = h$, and there is no flux on the sidewalls.

II. A BOUND ON THE VARIANCE

The suppression of concentration variance is a reasonable measure of the efficiency of mixing since in the absence of sources it decays due to diffusive mixing and it vanishes when complete homogenization is achieved. The variance is also a useful measure in the context of open flows [13–15]. We use techniques developed in [2–6] to bound the time-averaged variance of the concentration of a passive scalar. We shall use both the variance and its square root, the standard deviation, but final results will usually be quoted in terms of the variance.

A. The model and definitions

Consider a fixed domain Γ, in which flows a fluid with incompressible velocity field $\boldsymbol{u}(\boldsymbol{x}, t)$. The fluid transports a diffusing passive scalar with concentration $\theta(\boldsymbol{x}, t)$ which is stirred to some degree of homogeneity within Γ. The concentration $\theta(\boldsymbol{x}, t)$ in the domain Γ obeys the advection-diffusion equation

$$\partial_t \theta + \boldsymbol{u} \cdot \nabla \theta = \kappa \Delta \theta. \tag{1}$$

The flux of $\theta(\boldsymbol{x}, t)$ is defined by

$$\boldsymbol{F} := \boldsymbol{u}\,\theta - \kappa \nabla \theta\,. \tag{2}$$

At the boundary $\partial\Gamma$ of the domain, we specify the normal flux $\boldsymbol{F} \cdot \hat{\boldsymbol{n}}$ as

$$(\boldsymbol{F} \cdot \hat{\boldsymbol{n}})(0, y, z) = \mathcal{F}_0(y, z), \quad (\boldsymbol{F} \cdot \hat{\boldsymbol{n}})(h, y, z) = \mathcal{F}_h(y, z), \quad (\boldsymbol{F} \cdot \hat{\boldsymbol{n}})_{\text{sidewalls}} = 0, \tag{3}$$

where the sidewalls are the curved sections in Fig. 1. We denote the horizontal flux $\mathcal{F}(\boldsymbol{x}) := \hat{\boldsymbol{x}} \cdot \boldsymbol{F}(\boldsymbol{x})$, and we will often write $\mathcal{F}_x(y, z)$ to mean $\mathcal{F}(x, y, z)$, as in the boundary condition (3) above. Note that there is considerable literature, and a long running debate, regarding the appropriate boundary conditions to use for open-flow systems [15–19]; we use a prescribed normal flux for mathematical expediency.

Multiply the advection-diffusion equation (1) by an arbitrary smooth test function $\varphi(\boldsymbol{x}, t)$ and integrate:

$$\int_\Gamma \varphi\, \partial_t \theta \,\mathrm{d}V + \int_\Gamma \varphi \nabla \cdot (\boldsymbol{u}\,\theta)\,\mathrm{d}V = \kappa \int_\Gamma \varphi \Delta \theta \,\mathrm{d}V \tag{4}$$

where $\mathrm{d}V = \mathrm{d}x\,\mathrm{d}y$ in 2D and $\mathrm{d}x\,\mathrm{d}y\,\mathrm{d}z$ in 3D. To obtain (4), we have also used the incompressibility condition $\nabla \cdot \boldsymbol{u} = 0$. Next follow a few integration by parts,

$$\partial_t \int_\Gamma \theta\,\varphi\,\mathrm{d}V - \int_\Gamma \theta \partial_t \varphi\,\mathrm{d}V + \int_\Gamma \nabla\cdot(\boldsymbol{u}\,\varphi\,\theta)\,\mathrm{d}V - \int_\Gamma \theta\,\nabla\cdot(\boldsymbol{u}\,\varphi)\,\mathrm{d}V \\ = \kappa\left(\int_\Gamma \nabla\cdot(\varphi\nabla\theta)\,\mathrm{d}V - \int_\Gamma \nabla\cdot(\theta\,\nabla\varphi)\,\mathrm{d}V + \int_\Gamma \theta\Delta\varphi\,\mathrm{d}V\right). \quad (5)$$

We collect on the right the boundary terms,

$$\partial_t \int_\Gamma \theta\,\varphi\,\mathrm{d}V - \int_\Gamma \theta\left(\partial_t\varphi + \nabla\cdot(\boldsymbol{u}\,\varphi) + \kappa\Delta\varphi\right)\mathrm{d}V = -\int_\Gamma \nabla\cdot(\varphi\,\boldsymbol{F} + \kappa\,\theta\,\nabla\varphi)\,\mathrm{d}V\,, \quad (6)$$

and turn them into a surface integral,

$$\mathrm{RHS} = -\int_{\partial\Gamma} (\varphi\,\boldsymbol{F} + \kappa\,\theta\,\nabla\varphi)\cdot\hat{\boldsymbol{n}}\,\mathrm{d}a\,, \quad (7)$$

where $\mathrm{d}a = \mathrm{d}y$ in 2D and $\mathrm{d}y\,\mathrm{d}z$ in 3D. On the sidewalls, we have $\boldsymbol{F}\cdot\hat{\boldsymbol{n}} = 0$ because of boundary conditions (3), so the flux term in (7) vanishes. Since we haven't solved the full problem (1), we don't know θ on the boundary. To remove the direct θ dependence in (7), we restrict attention to test functions φ with

$$\nabla\varphi\cdot\hat{\boldsymbol{n}} = 0 \quad \text{on} \quad \partial\Gamma. \quad (8)$$

All that remains of the integral (7) are the surfaces at $x = 0$ and $x = h$, and Eq. (6) is then

$$\partial_t \int_\Gamma \theta\,\varphi\,\mathrm{d}V + \langle\theta\,\mathcal{L}^*\varphi\rangle = \int_{\partial\Gamma_0} \varphi\,\mathcal{F}_0\,\mathrm{d}a - \int_{\partial\Gamma_h} \varphi\,\mathcal{F}_h\,\mathrm{d}a, \quad (9)$$

with $\mathrm{d}a = \mathrm{d}y$ in 2D and $\mathrm{d}y\,\mathrm{d}z$ in 3D, and $\partial\Gamma_x$ is the cross-section at constant x. We also defined the formal adjoint of the advection-diffusion operator,

$$\mathcal{L}^*\varphi \coloneqq -\partial_t\varphi - \nabla\cdot(\boldsymbol{u}\,\varphi) - \kappa\Delta\varphi\,. \quad (10)$$

Equation (9) is the fundamental 'integrated equation' that we will be using subsequently. Setting $\varphi = 1$ in (9), we get an equation for the conservation of total θ,

$$\partial_t \int_\Gamma \theta\,\mathrm{d}V = \int_{\partial\Gamma_0} \mathcal{F}_0\,\mathrm{d}a - \int_{\partial\Gamma_h} \mathcal{F}_h\,\mathrm{d}a \quad (11)$$

which of course says that the change in $\int_\Gamma \theta\,\mathrm{d}V$ is the net difference in fluxes at $x = 0$ and $x = h$. For the remainder of the paper, we shall consider the case where

$$\int_{\partial\Gamma_0} \mathcal{F}_0\,\mathrm{d}a = \int_{\partial\Gamma_h} \mathcal{F}_h\,\mathrm{d}a = 0 \quad (12)$$

so that the total amount of θ in Γ is always 0.

B. Lower bound on the variance

We define angle brackets and overbars as

$$\langle f \rangle \coloneqq \lim_{T\to\infty} \frac{1}{T} \int_0^T \mathrm{d}t \int_\Gamma f(\boldsymbol{x},t)\ \mathrm{d}V, \qquad \overline{f} \coloneqq \lim_{T\to\infty} \frac{1}{T} \int_0^T \mathrm{d}t \int_{\partial\Gamma_x} f(\boldsymbol{x},t)\,\mathrm{d}a. \tag{13}$$

(The limits are assumed to converge.) After time-integrating Eq. (9) the term $\langle \partial_t(\varphi\,\theta)\rangle$ vanishes and we have

$$\langle \theta\,\mathcal{L}^*\varphi\rangle = \overline{(\varphi\,\mathcal{F} + \kappa\,\theta\,\partial_x\varphi)}\Big|_0 - \overline{(\varphi\,\mathcal{F} + \kappa\,\theta\,\partial_x\varphi)}\Big|_h\,. \tag{14}$$

The notation $\overline{f}\big|_c$ signifies $\overline{f}$ evaluated at $x = c$. The conservation equation (11) implies $\langle\theta\rangle = 0$, so the spatially-integrated variance of the concentration field is $\langle\theta^2\rangle$. We shall omit the qualifier 'spatially-integrated' most of the time.

Using the Cauchy–Schwartz inequality, we can extract from (14) a bound on the standard deviation,

$$\langle\theta^2\rangle^{1/2} \geq \frac{\left|\left(\overline{\varphi\,\mathcal{F}}\big|_0 - \overline{\varphi\,\mathcal{F}}\big|_h\right)\right|}{\langle|\mathcal{L}^*\varphi|^2\rangle^{1/2}}\,. \tag{15}$$

The right-hand side of the bound (15) contains only known quantities. The bound says that for given functions $\boldsymbol{u}$, $\mathcal{F}_0 \coloneqq \mathcal{F}|_0$, $\mathcal{F}_h \coloneqq \mathcal{F}|_h$, and diffusivity κ, the passive scalar must exhibit a minimum level of fluctuations. Since better mixing requires decreasing fluctuations, Eq. (15) is a rigorous bound on the potential efficiency of a mixer. In practice, one tries to find a function φ to make the bound as sharp as possible, that is to maximize the right-hand side of (15). The optimal φ will, in principle, depend on all the problem parameters.

Observe that adding a constant c to φ changes the numerator in (15) by a factor $c\,(\overline{\mathcal{F}_0} - \overline{\mathcal{F}_h})$, which vanishes because the total amount of θ within the domain is conserved (after the long-time averaging). Hence, adding a constant to φ does not affect the estimate.

If we have a semi-infinite 'channel,' with $h \to \infty$, then the scalar field at h will become completely homogeneous due to diffusion ($\theta \to 0$) and its flux will necessarily vanish. We then have

$$\langle\theta^2\rangle^{1/2} \geq \frac{\left|\left(\overline{\varphi\,\mathcal{F}}\big|_0\right)\right|}{\langle|\mathcal{L}^*\varphi|^2\rangle^{1/2}}\,. \tag{16}$$

Equation (16) is ideal for this channel configuration, since we only require knowledge of the flux at $x = 0$. (Alternatively, we could also obtain (16) by specifying $\varphi = 0$ at $x = h$.) We shall focus exclusively on the semi-infinite channel configuration ($h \to \infty$) for the remainder of the paper.

C. A bound for all flows

The bound (16) requires complete knowledge of the velocity field $\boldsymbol{u}$. However, we can turn it into a 'global' bound over all allowable velocity fields. For simplicity, from now on we restrict attention to a uniform, rectangular cross section of dimensions L_y and L_z, and to a time-independent velocity field.

First we bound the numerator in (16). For a time-independent test function φ,

$$\langle|\mathcal{L}^*\varphi|^2\rangle = \langle|\boldsymbol{u}\cdot\nabla\varphi + \kappa\Delta\varphi|^2\rangle \leq 2\langle|\boldsymbol{u}\cdot\nabla\varphi|^2\rangle + 2\kappa^2\langle|\Delta\varphi|^2\rangle. \tag{17}$$

We bound the first term in (17),

$$\begin{aligned} 2\langle|\boldsymbol{u}\cdot\nabla\varphi|^2\rangle &\le 2\int_0^\infty \overline{|\boldsymbol{u}|^2|\nabla\varphi|^2}\,\mathrm{d}x \\ &\le 2\int_0^\infty \overline{|\boldsymbol{u}|^2}\sup_{y,z}|\nabla\varphi|^2\,\mathrm{d}x \\ &\le 2\sup_x \overline{|\boldsymbol{u}|^2}\int_0^\infty \sup_{y,z}|\nabla\varphi|^2\,\mathrm{d}x = 2U^2L^{d-2}\,c_1 \end{aligned}$$

where we defined the mixing flow velocity scale $U \ge 0$ by

$$U^2 := L^{1-d}\sup_x \overline{|\boldsymbol{u}|^2} \tag{18}$$

and the length scale $L := \sqrt{L_yL_z}$ in 3D, or $L := L_y$ in 2D. We also defined the dimensionless coefficient

$$c_1\{\varphi\} := L\int_0^\infty \sup_{y,z}|\nabla\varphi|^2\,\mathrm{d}x\,. \tag{19}$$

We define another dimensionless coefficient

$$c_2\{\varphi\} := L^{4-d}\,\langle|\Delta\varphi|^2\rangle \tag{20}$$

which, using (17), allows us to write

$$\langle|\mathcal{L}^*\varphi|^2\rangle \le 2U^2L^{d-2}\,c_1 + 2\kappa^2L^{d-4}\,c_2 = 2\kappa^2L^{d-4}\left(c_1\,\mathrm{Pe}^2 + c_2\right) \tag{21}$$

where the Péclet number is defined as

$$\mathrm{Pe} := UL/\kappa. \tag{22}$$

Now we examine the numerator in (16). The flux $\mathcal{F}$ has units of velocity (considering without loss of generality that θ is dimensionless), so we can define the dimensionless coefficient

$$c_3\{\varphi,\mathcal{F}_0\} := U^{-1}L^{1-d}\,\left|(\overline{\varphi\,\mathcal{F}}\big|_0)\right|\,. \tag{23}$$

Combining the results we can write the bound as

$$\langle\theta^2\rangle^{1/2} \ge L^{d/2}\frac{c_3\,\mathrm{Pe}}{\sqrt{2(c_1\,\mathrm{Pe}^2+c_2)}}\,, \tag{24}$$

where now the properties of the stirring flow only appear as the scale U in Pe. For small or large Pe, we can improve the bound a little by neglecting the appropriate term in (17), which allows us to leave out the factor of 2 in that equation. We then get the asymptotic estimates

$$\langle\theta^2\rangle^{1/2} \gtrsim \begin{cases} L^{d/2}\,(c_3/\sqrt{c_2})\,\mathrm{Pe}\,, & \mathrm{Pe}\ll 1; \\ L^{d/2}\,(c_3/\sqrt{c_1}), & \mathrm{Pe}\gg 1. \end{cases} \tag{25}$$

For convenience of display, we combine the asymptotic bounds (25) into the same form as (24),

$$\langle\theta^2\rangle^{1/2} \gtrsim L^{d/2}\frac{c_3\,\mathrm{Pe}}{\sqrt{c_1\,\mathrm{Pe}^2+c_2}}\,, \quad \mathrm{Pe}\ll 1 \text{ or } \mathrm{Pe}\gg 1, \tag{26}$$

where it is understood that this estimate is only valid asymptotically for small or large Pe. For our purposes, the error made at intermediate Pe will be small.

The small Pe bound says that the standard deviation can become small in that case: this is the diffusion-dominated limit. For large Pe, the lower bound saturates and becomes independent of Pe: we shall examine this behavior more closely in Section IV, and see if it can be realized in practice.

D. Choosing the test function φ

To get usable numbers out of (26) we need to choose φ for a given $\mathcal{F}_0$. We specialize to two dimensions ($d = 2$) and

$$\mathcal{F}_0(y) = UH \sin qy\,, \tag{27}$$

where the constant H is a dimensionless measure of the flux. We consider periodic boundary conditions in y, which for our purposes is equivalent to the no-flux conditions on the sidewalls in (3). The wavenumber $q = Q/L$, where Q is an integer multiple of 2π and $L = L_y$.

To get the sharpest bound, our goal is to maximize the right-hand side of (26) as much as possible. Hence we need a test function φ with a large projection on $\mathcal{F}_0$, to maximize c_3. The most expedient approach is to take a separable form for φ with the y dependence mimicking $\mathcal{F}_0$'s:

$$\varphi = \Phi(x)\, \sin qy, \qquad \Phi(0) = 1. \tag{28}$$

We can then easily compute

$$c_3 = U^{-1}L^{-1}\,\Phi(0)\,UH \int_0^L \sin^2 qy\,\mathrm{d}y = \tfrac{1}{2}H. \tag{29}$$

and

$$c_2 = L^2\,\langle|\Delta\varphi|^2\rangle = L^2\,\langle|(\Phi'' - q^2\Phi)\sin qy|^2\rangle = \tfrac{1}{2}L^3 \int_0^\infty |\Phi'' - q^2\Phi|^2\,\mathrm{d}x\,. \tag{30}$$

The constant c_1 is more problematic, since we need to evaluate the supremum inside the integral:

$$c_1 = L\int_0^\infty \sup_y |\nabla\varphi|^2\,\mathrm{d}x = L\int_0^\infty \sup_y \left((\Phi')^2\sin^2 qy + q^2\Phi^2\cos^2 qy\right)\,\mathrm{d}x\,. \tag{31}$$

To find the supremum, take the derivative and set to zero,

$$\frac{d}{dy}\left((\Phi')^2\sin^2 qy + q^2\Phi^2\cos^2 qy\right) = \left((\Phi')^2 - q^2\Phi^2\right) q\sin 2qy = 0. \tag{32}$$

We need only consider the extrema at $qy = 0$ and $\pi/2$, since $\sin 2qy$ function is π-periodic, which leads to

$$c_1 = L\int_0^\infty \max\left(q^2\Phi^2\,,\,\Phi'^2\right)\,\mathrm{d}x\,. \tag{33}$$

Now we make specific choices for Φ. Consider first the limit of small Pe. In that case we ignore c_1 and try to minimize c_2. The Euler–Lagrange equation for (30) is

$$\Phi'''' - 2q^2\Phi'' + q^4\Phi = 0. \tag{34}$$

The appropriately integrable solution that also satisfies $\Phi(0) = 1$, $\Phi'(0) = 0$ is

$$\Phi(x) = (1 + qx)\, \mathrm{e}^{-qx} \tag{35}$$

which gives $c_2 = (qL)^3 = Q^3$.

Conversely, for large Pe we ignore c_2 and focus on c_1. In that case, we might like to use the function $\Phi = \mathrm{e}^{-qx}$, for which $\Phi' = -q\Phi$, so the two choices for the max in (33) are the same, and $c_1 = \frac{1}{2}(qL) = \frac{1}{2}Q$ for the constant. The only problem is that this choice for Φ does not satisfy the boundary condition $\Phi'(0) = 0$. This is easily remedied by inserting a small boundary layer near $x = 0$, and letting the size of the layer go to zero. For large Pe, the correction incurred can be neglected.

We can combine our two asymptotic results as in (26) to conclude

$$\frac{1}{LH}\, \langle \theta^2 \rangle^{1/2} \gtrsim \frac{\mathrm{Pe}}{2\sqrt{\frac{1}{2}Q\, \mathrm{Pe}^2 + Q^3}}\,, \qquad \mathrm{Pe} \ll 1 \text{ or } \mathrm{Pe} \gg 1. \tag{36}$$

This estimate is rigorous for large and small Pe, and we expect that error made at intermediate Pe is typically small. This is illustrated by the example developed in the next section.

III. EXAMPLE: THE BARBERPOLE FLOW MIXER

As an illustration of typical features of open-flow systems, we study a toy problem that can be solved exactly. We will then compare the exact standard deviation to the bound (36). We consider the 2D spatially uniform flow

$$\boldsymbol{u} = u\, \hat{\boldsymbol{x}} + v\, \hat{\boldsymbol{y}}\,, \tag{37}$$

where u and v are constants. We we solve the steady advection-diffusion equation for $\theta(\boldsymbol{x})$, where $\boldsymbol{x} = (x, y) \in \Gamma = [0, \infty) \times [0, L_y]$, with periodic boundary conditions in y and the flux (2) specified as

$$\hat{\boldsymbol{x}} \cdot \boldsymbol{F}(0, y) = \mathcal{F}_0(y), \qquad \boldsymbol{F}(x, y) \to 0 \quad \text{as} \quad x \to \infty. \tag{38}$$

For the case of pure advection, with $\kappa = 0$ in Eq. (1), the solution is

$$\theta(x, y) = u^{-1} \mathcal{F}_0\left(y - x\, v/u\right)\,. \tag{39}$$

The concentration has a 'barberpole' pattern (see Fig. 2): the imposed distribution at $x = 0$ is twisted around the periodic direction y, with the tilt angle γ determined by the ratio of v and u. The cross-sectional variance $\overline{\theta^2}/L_y$ is independent of x, and there is no mixing, as expected.

A. Advection and diffusion

Now we include diffusion in Eq. (1). We first Fourier-expand in y,

$$\theta(x, y) = \sum_q \theta_q(x)\, \mathrm{e}^{\mathrm{i}qy} + \text{c.c.} \tag{40}$$

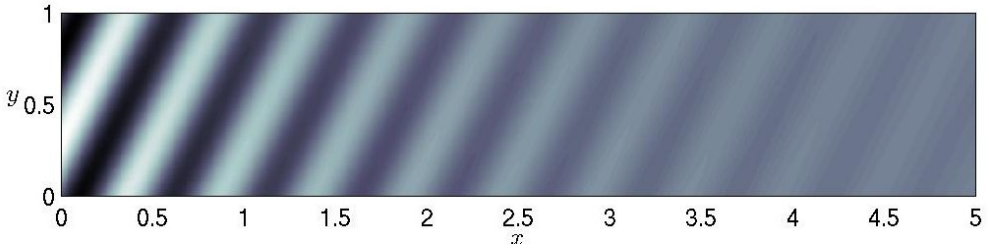

FIG. 2: Concentration field $\theta(\boldsymbol{x})$ for the barberpole flow (parameters values are $H = 1$, $\mathrm{Pe} = 100$, $\gamma = 3\pi/8$, $L = L_y = 1$).

where q is an integer multiple of $2\pi/L_y$. In the steady case, the advection-diffusion equation (1) for the amplitude of the vertical mode q becomes

$$\kappa\theta_q'' - u\,\theta_q' - q(\kappa q + \mathrm{i}\,v)\theta_q = 0. \tag{41}$$

Using the length scale $L = L_y$ and velocity scale $U = \sqrt{u^2 + v^2}$ (consistent with the definitions in Section II C), we define the rescaled variables $X = x/L$, $Y = y/L$, $Q = qL$, and $\Theta(X) = \theta_q(LX)$ to get the dimensionless ODE

$$\Theta'' - \mathrm{Pe}\,\cos\gamma\,\Theta' - Q(Q + \mathrm{i}\,\mathrm{Pe}\,\sin\gamma)\Theta = 0 \tag{42}$$

where the pitch angle γ is defined by $\tan\gamma = v/u$ and the Péclet number Pe is as in Eq. (22). This has solution

$$\Theta(X) = \Theta(0)\,\mathrm{e}^{-(\nu+\mathrm{i}\omega)X}, \qquad X \geq 0, \tag{43}$$

where we defined the spatial decay rate by

$$\nu = \alpha - \tfrac{1}{2}\mathrm{Pe}\,\cos\gamma \tag{44}$$

with

$$\alpha = \sqrt{\tfrac{1}{2}\left(R^2 + \left(\tfrac{1}{4}\,\mathrm{Pe}^2\cos^2\gamma + Q^2\right)\right)}, \qquad \omega = \sqrt{\tfrac{1}{2}\left(R^2 - \left(\tfrac{1}{4}\,\mathrm{Pe}^2\cos^2\gamma + Q^2\right)\right)},$$
$$R^2 = \sqrt{Q^2\,\mathrm{Pe}^2\sin^2\gamma + \left(\tfrac{1}{4}\,\mathrm{Pe}^2\cos^2\gamma + Q^2\right)^2}\,.$$

We have $\nu > 0$ since $\alpha \geq \left(\frac{1}{4}\,\mathrm{Pe}^2\cos^2\gamma + Q^2\right)^{1/2} > \frac{1}{2}\,\mathrm{Pe}\,\cos\gamma$; hence, the solution (43) decays with X, as required. Using the form (27) for the flux $\mathcal{F}_0(y)$ and the boundary condition (38),

$$\mathcal{F}_0(y) = UH\sin qy = \mathcal{F}(0,y) = \frac{\kappa}{L}\left(\mathrm{Pe}\,\cos\gamma + (\nu + \mathrm{i}\omega)\right)\Theta(0)\,\mathrm{e}^{\mathrm{i}qy} + \text{c.c.} \tag{45}$$

which we can use to solve for

$$\Theta(0) = \frac{1}{2\mathrm{i}}\,\frac{H\,\mathrm{Pe}}{\mathrm{Pe}\,\cos\gamma + \nu + \mathrm{i}\omega}\,. \tag{46}$$

Figure 2 shows the concentration field pattern for the parameter values $H = 1$, $Q = 2\pi$, $\mathrm{Pe} = 100$, $\gamma = 3\pi/8$, $L = L_y = 1$. The tilted stripes make an angle γ with the horizontal, and the intensity decays in space at a rate ν.

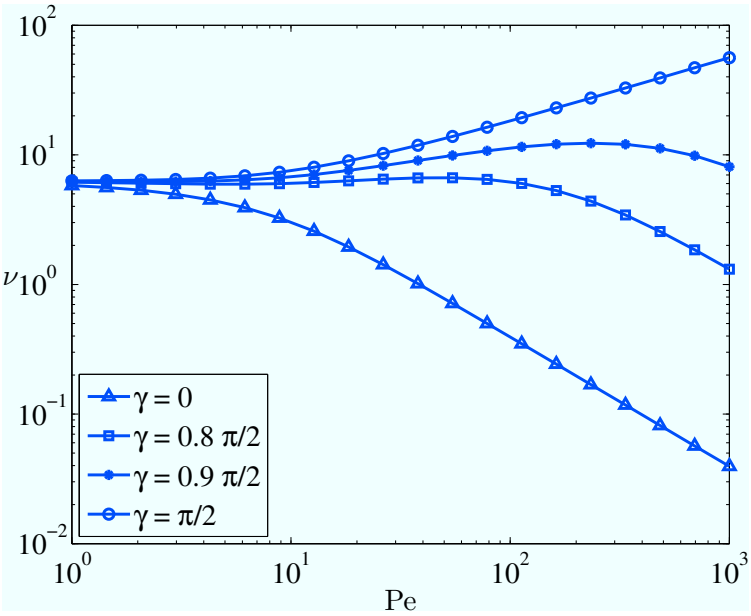

FIG. 3: Decay rate ν from Eq. (44) for the barberpole flow, as a function of Pe. For any value of $\gamma < \pi/2$, the decay rate ultimately goes to zero like Pe^{-1} for $\mathrm{Pe} \gg 1$. However, for $\gamma = \pi/2$ the decay rate grows as $\mathrm{Pe}^{1/2}$.

For small Pe, we have the expansions

$$\nu = Q - \tfrac{1}{2}\mathrm{Pe}\,\cos\gamma + \mathrm{O}\big(\mathrm{Pe}^2\big)\,, \qquad \omega = \tfrac{1}{2}\mathrm{Pe}\,\sin\gamma + \mathrm{O}\big(\mathrm{Pe}^3\big)\,. \tag{47}$$

To leading order in Pe, the spatial decay rate ν is independent of Pe and the pitch angle γ. This is because in the absence of flow (or for a weak flow) the decay scale length is set by q, and the diffusivity completely drops out.

For large Pe, we have the expansions

$$\nu = Q^2\sec^3\gamma\,\mathrm{Pe}^{-1} + \mathrm{O}\big(\mathrm{Pe}^{-3}\big)\,, \qquad \omega = Q\tan\gamma + \mathrm{O}\big(\mathrm{Pe}^{-2}\big)\,. \tag{48}$$

These are valid for γ not too close to $\pi/2$. Figure 3 shows the spatial decay rate ν as function of Pe, for several values of γ. For large Pe, the decay rate ultimately decays as Pe^{-1}. However, for $\gamma = 0$ the decay rate *grows* as $\mathrm{Pe}^{1/2}$. This case corresponds to no horizontal flow: the vertical flow is very effective at pushing the source onto the sink, leading to fast spatial decay. But the flux into the mixing region is then entirely due to diffusion, so this is not a very practical situation. We will discuss this case further in Section III B. Another striking feature of the curve in Fig. 3 is that some curves have a local maximum.

The enhancement to the decay rate is related to shear or Taylor dispersion, in the sense that it arises from the tilting of concentration contours. However, here it is not due to shear, but to the cross-velocity v.

B. Computing the variance

For a single Fourier mode, the variance integrated over a cross-section is

$$\overline{\theta^2} = \int_0^{L_y} \theta^2\,\mathrm{d}y = 2L\,|\Theta(X)|^2 = 2L\,|\Theta(0)|^2\,\mathrm{e}^{-2\nu X}, \tag{49}$$

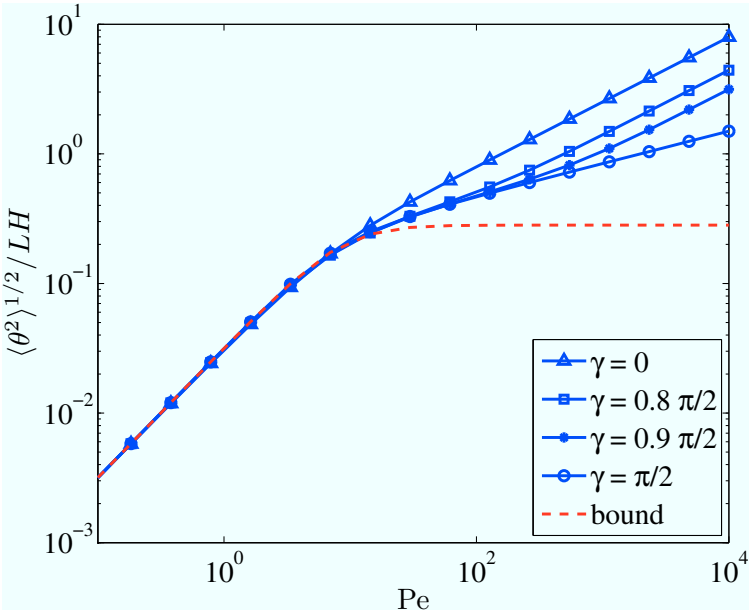

FIG. 4: Comparison of the standard deviation of the concentration field for the barberpole mixer (solid lines) and the global (lower) bound (26) for all flows. For small Pe, all the curves are linear in Pe. For large Pe, the barberpole solutions scale as $\mathrm{Pe}^{1/2}$, unless $\gamma = \pi/2$ for which the scaling is $\mathrm{Pe}^{1/4}$.

and the total variance in the domain $\Gamma = [0, \infty) \times [0, L_y]$ is

$$\langle\theta^2\rangle = \int_0^\infty 2L\,|\Theta(0)|^2\,\mathrm{e}^{-2\nu X}\,\mathrm{d}x = L^2\,\frac{1}{\nu}\,|\Theta(0)|^2\,, \tag{50}$$

or in term of the standard deviation

$$\frac{1}{LH}\,\langle\theta^2\rangle^{1/2} = \frac{\mathrm{Pe}}{2\sqrt{\nu}\sqrt{(\mathrm{Pe}\,\cos\gamma+\nu)^2+\omega^2}}\,. \tag{51}$$

For small Péclet number, the standard deviation is

$$\frac{1}{LH}\,\langle\theta^2\rangle^{1/2} = \frac{\mathrm{Pe}}{2Q^{3/2}} - \frac{\mathrm{Pe}^2\,\cos\gamma}{8q^{5/2}} + \mathrm{O}\big(\mathrm{Pe}^3\big)\,, \qquad \mathrm{Pe} \ll 1, \tag{52}$$

whilst for large Pe it has the form

$$\frac{1}{LH}\,\langle\theta^2\rangle^{1/2} = \frac{1}{2Q}\,\sqrt{\mathrm{Pe}\,\cos\gamma} + \mathrm{O}\Big(\mathrm{Pe}^{-3/2}\Big)\,, \qquad \mathrm{Pe} \gg 1. \tag{53}$$

If $\gamma = \pi/2$, then the $\mathrm{O}\Big(\mathrm{Pe}^{3/2}\Big)$ term in the large Pe expression diverges, and we have

$$\frac{1}{LH}\,\langle\theta^2\rangle^{1/2} = \left(\frac{\mathrm{Pe}}{8Q^3}\right)^{1/4} + \mathrm{O}\Big(\mathrm{Pe}^{-3/4}\Big)\,, \qquad \mathrm{Pe} \gg 1,\ \gamma = \pi/2. \tag{54}$$

These scalings are evident in Fig. 4, which compares the exact standard deviation (51) to the bound (36). For small Pe the exact standard deviation and the bound are both linear in

Pe. For large Pe the lower bound flattens out and becomes independent of Pe. The closest the exact standard deviation for the barberpole flow comes to the theoretical lower bound is for $\gamma = \pi/2$, since then the exact result scales like $\mathrm{Pe}^{1/4}$. For any other value of $\gamma < \pi/2$ the $\mathrm{Pe}^{1/4}$ scaling holds for a short while, but eventually rises as $\mathrm{Pe}^{1/2}$ when $\mathrm{Pe}\cos\gamma$ becomes large. Hence, the 'optimal' barberpole flow is one for which the horizontal flow u vanishes ($\gamma = \pi/2$): in that case all of the velocity field is devoted to pushing the source onto the sink, in a manner similar to the optimal flows found for closed systems [4, 7]. However, unlike the closed systems this flow does not scale optimally: the bound suggests that there could exist a flow producing a shallower scaling. We will discuss the possibility that such flows exist in Section IV. Note also that as mentioned in Section III A the flow with $\gamma = \pi/2$ is very singular: the scalar flux into the domain is entirely due to diffusion, so there is no *mass* flux into the mixing region. This is not a very realistic concept on which to build an industrial mixer.

IV. EXAMPLE: A MEANDERING FLOW MIXER

The barberpole flow of Section III is a nice model because of its exact solvability but it has some undesirable pathologies. Most importantly it is hard to relate it to practical situations where a channel flow enters and then exits a well-defined 'mixing region,' where mechanical stirring occurs and most of the mixing takes place. A better example would involve a flow that varies in x.

As a more general version of the constant barberpole flow (37), we now consider the case for which the $\hat{\boldsymbol{y}}$ component is a functions of x,

$$\boldsymbol{u}(x) = u\,\hat{\boldsymbol{x}} + v(x)\,\hat{\boldsymbol{y}} \tag{55}$$

with $u > 0$. The domain and boundary conditions are as in Section III. This is a 'meandering' velocity field that changes its direction with x but never backtracks. Once again we Fourier expand as in (40) and focus on a single mode $\theta_q(x)$. The equation to solve is still (41) but with $v(x)$ nonconstant. Unlike the constant flow case, we cannot solve the equation in full generality, but since we are mostly interested in the small κ case the WKBJ method allows us to get an explicit approximate solution. We assume the standard WKBJ ansatz

$$\theta_q(x) = \theta_q(0)\,\exp(S(x)) = \theta_q(0)\,\exp(S_0(x) + \kappa\,S_1(x) + \cdots) \tag{56}$$

where $S(0) = 0$, and to save notation we left out a q subscript on S. After inserting into (41) and collecting terms in κ, we can easily solve for the first two terms,

$$S_0(x) = -\mathrm{i}\,\frac{q}{u}\int_0^x v(\xi)\,\mathrm{d}\xi\,, \tag{57a}$$

$$S_1(x) = -\frac{q^2 x}{u} - \mathrm{i}\frac{q}{u^2}(v(x) - v(0)) - \frac{q^2}{u^3}\int_0^x v^2(\xi)\,\mathrm{d}\xi\,. \tag{57b}$$

We will not be finding higher-order terms, and thus decree $S = S_0 + S_1$; it will prove more convenient to decompose this into real and imaginary parts as $S(x) = S_\mathrm{r}(x) + \mathrm{i}\,S_\mathrm{i}(x)$, with

$$S_\mathrm{r}(x) = -\frac{\kappa q^2}{u^3}\left(u^2 x + \int_0^x v^2(\xi)\,\mathrm{d}\xi\right), \tag{58a}$$

$$S_\mathrm{i}(x) = -\frac{q}{u}\int_0^x v(\xi)\,\mathrm{d}\xi - \frac{\kappa q}{u^2}(v(x) - v(0))\,. \tag{58b}$$

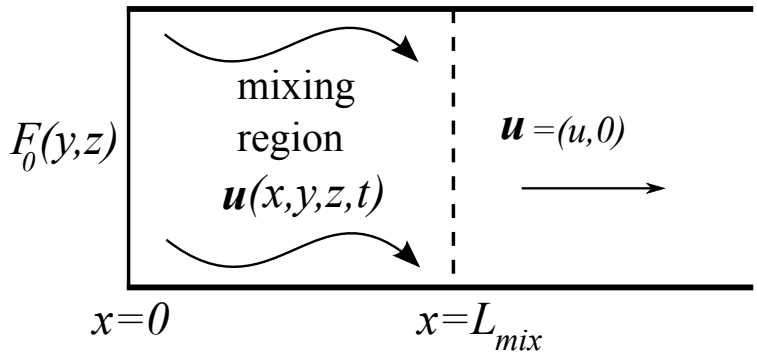

FIG. 5: The domain for the meandering flow: within the mixing region the flow takes the form (55), and for $x > L_{\rm mix}$ it has the simpler, constant form $(u, 0)$.

Now we need to apply boundary conditions at $x = 0$, where the flux is

$$\mathcal{F}(0, y) = \theta_q(0)\,(u - \kappa S'(0))\,\mathrm{e}^{\mathrm{i}qy} + \text{c.c.} = UH \sin qy \tag{59}$$

where we used $S(0) = 0$. We use this to solve for

$$\theta_q(0) = \frac{UH}{2\mathrm{i}\,(u - \kappa S'(0))}\,. \tag{60}$$

Note that the derivative in S' simply annuls the integrals in the definition of S, so this prefactor only involves the unintegrated velocity field at $x = 0$. The variance integrated over a cross-section for a single Fourier mode is

$$\overline{\theta^2} = \int_0^{L_y} \theta^2\,\mathrm{d}y = 2L_y\,|\theta_q(0)|^2\,\mathrm{e}^{2S_{\rm r}(x)}, \tag{61}$$

with

$$|\theta_q(0)| = \frac{UH}{2\sqrt{(u - \kappa S'_{\rm r}(0))^2 + (\kappa S'_{\rm i}(0))^2}}\,. \tag{62}$$

Thus $S_{\rm r}(x)$ characterizes the spatial decay of the concentration field with x. The total, spatially-integrated variance is

$$\langle\theta^2\rangle = 2L_y\,|\theta_q(0)|^2 \int_0^\infty \mathrm{e}^{2S_{\rm r}(x)}\,\mathrm{d}x. \tag{63}$$

To make further progress we will now assume that we have a mixing region localized in x of length $L_{\rm mix}$, extending from $0 < x \le L_{\rm mix}$ (see Fig. (5)). Before and after that region we have $v = 0$ as well as $v'(0) = 0$. In that case $S'(0) = S'_{\rm r}(0) = -\kappa q^2/u$. As for the integral in (63), it splits as

$$\int_0^\infty \mathrm{e}^{2S_{\rm r}(x)}\,\mathrm{d}x = \int_0^{L_{\rm mix}} \mathrm{e}^{2S_{\rm r}(x)}\,\mathrm{d}x + \int_{L_{\rm mix}}^\infty \mathrm{e}^{-2\kappa q^2 x/u}\,\mathrm{d}x\,. \tag{64}$$

Since $S_{\rm r} \sim \kappa$ is assumed small, the first integral is roughly equal to $L_{\rm mix}$ and the second integral can be done exactly, yielding

$$\int_0^\infty \mathrm{e}^{2S_{\rm r}(x)}\,\mathrm{d}x \simeq L_{\rm mix} + \frac{u}{2\kappa q^2}\,\mathrm{e}^{-2\kappa q^2 L_{\rm mix}/u}\,. \tag{65}$$

We already assumed that $\kappa q^2 L_{\mathrm{mix}}/u$ was small in approximating the first integral by L_{mix}, so we do it again in the exponential term to find after expanding

$$\int_0^\infty \mathrm{e}^{2S_{\mathrm{r}}(x)}\,\mathrm{d}x \simeq \frac{u}{2\kappa q^2}\,. \tag{66}$$

Neglecting the κ in the denominator of (62), we combine it with (66) in (63) to find

$$\langle\theta^2\rangle \simeq 2L_y \frac{U^2H^2}{4\,u^2}\,\frac{u}{2\kappa q^2} = L_y \frac{U^2H^2}{4\,u\kappa q^2}\,. \tag{67}$$

Recall the definition of U, Eq. (18): outside the mixing region we have $\overline{|\boldsymbol{u}|^2}/L_y = u^2$, but inside we have $\overline{|\boldsymbol{u}|^2}/L_y \geq u^2$ because of the extra stirring motion. Hence, we put $u = c_4^{-2}\,U$, with $c_4 \geq 1$, and obtain

$$\frac{1}{LH}\,\langle\theta^2\rangle^{1/2} \simeq \frac{c_4}{2Q}\,\mathrm{Pe}^{1/2} \tag{68}$$

where the length scale $L = L_y$ and $Q = qL_y$. For a constant flow, we have $c_4 = 1$ and we recover the asymptotic form (53) with $\gamma = 0$. The constant $c_4 \gtrsim 1$ measures the vigor of stirring within the mixing region as compared with the mean flow.

The standard deviation paradoxically appears to increase with c_4: this is an artifact of our dimensionless scaling, which was natural for the bounding approach of Section II C but is less appropriate here. If instead we normalize the flux as $\mathcal{F}_0(y) = uH_\infty \sin qy$, where H_∞ now measures the flux normalized by the inflow/outflow velocity u, we find

$$\langle\theta^2\rangle \simeq 2L_y \frac{u^2H_\infty^2}{4\,u^2}\,\frac{u}{2\kappa q^2} = L_y \frac{uH_\infty^2}{4\kappa q^2}\,, \tag{69}$$

or

$$\frac{1}{LH_\infty}\,\langle\theta^2\rangle^{1/2} \simeq \frac{1}{2Q}\,\mathrm{Pe}_\infty^{1/2}, \qquad \mathrm{Pe}_\infty \coloneqq \frac{u\,L}{\kappa}. \tag{70}$$

So if we use a Péclet number based on the inflow, the variance is completely independent of the stirring flow, at leading order in Pe_∞. The stirring is too weak to change not just the $\mathrm{Pe}_\infty^{1/2}$ scaling, but also the prefactor. This might seem surprising but is actually rather obvious: we assumed in calculating Eqs. (68) and (70) that the small diffusion dominated even in the mixing region. This is justified since the flow is 2D and steady, so chaotic advection cannot occur [20]. Hence the finite mixing region does not decrease the variance enough, and the total variance is dominated by the infinite region $x > L_{\mathrm{mix}}$.

The scaling (68) for the general 'meandering flow' shows that there is no hope of approaching the lower bound Pe^0 scaling with such a flow. Let us assume that the fluid gets well-mixed in the mixing region, in a diffusion-independent way as occurs for chaotic and turbulent mixing. Then the first term in integral (64) yields a diffusion-independent constant L_{mix}, and the second term can be neglected. The variance Eq. (67) becomes

$$\langle\theta^2\rangle \simeq 2L_y \frac{u^2H_\infty^2}{4\,u^2}\,L_{\mathrm{mix}}\,, \tag{71}$$

which leads to the standard deviation

$$\frac{1}{LH_\infty}\,\langle\theta^2\rangle^{1/2} \simeq \tfrac{1}{2}(L_{\mathrm{mix}}/L)^{1/2}. \tag{72}$$

This indeed exhibits a Pe-independent scaling. We emphasize that the difference between (72) and (70) is that the former assumes that the length of mixing region required to reduce the variance to a certain level becomes independent of the diffusivity as κ becomes smaller, which is a standard assumption of turbulent and chaotic mixing. (In fact, typically there will be a weak logarithmic correction to $L_{\rm mix}$, having to do with the length needed to create small scales.) In any case it remains an open challenge to produce an explicit flow that realizes such optimal mixing.

V. SUMMARY

We have proposed a framework for the theoretical investigation of questions of mixing efficiency in open flows with passive scalar tracer concentration variations sustained by sources and sinks at an inlet. The measure we used to gauge the effectiveness of the stirring is the spatio-temporal variance of the scalar concentration, a quantity that can be analyzed via the advection-diffusion equation. We derived lower bounds on the variance that are observed to be sharp at low Péclet number (weak stirring) and to capture the qualitative trend at high Péclet number (strong stirring) for a particular model problem, the "barberpole" flow. Concentration variations introduced at an inlet and subsequently swept downstream are likely most effectively stirred (for the mixing criterion adopted here) by flows that, in a downstream moving frame, provide the kind of chaotic mixing known to work well for transient mixing problems. It remains an open question to determine if such a flow can be designed or characterized in detail even for the simple idealized model considered here.

Many other questions remain open as well. How does the mixing efficiency of a given flow vary as the inlet source varies? How does the mixing efficiency depend on the length scales we choose to focus on? For example the gradient variance or some other norm might just as well be invoked as the gauge to measure mixing efficiency. This issue is known to be important for mixing tracer fluctuations injected via steady bulk sources and sinks, where the dependence of the mixing measures on the the Péclet number depends explicitly on the length scales in the sources, the sinks, and those chosen for the mixing measure [3–5]. These questions remain for future investigations.

Acknowledgments

The authors are grateful to W. R. Young for helpful discussions, and to the hospitality of the Institute for Mathematics and its Applications (supported by NSF). CRD was supported by NSF under grants PHY-0555324 and PHY-0855335, and J-LT under grant DMS-0806821.

[1] L. N. Howard, 'Heat transport by turbulent convection,' *J. Fluid Mech.* **17**, 405 (1963).

[2] J.-L. Thiffeault, C. R. Doering, and J. D. Gibbon, 'A bound on mixing efficiency for the advection–diffusion equation,' *J. Fluid Mech.* **521**, 105–114 (2004).

[3] C. R. Doering and J.-L. Thiffeault, 'Multiscale mixing efficiencies for steady sources,' *Phys. Rev. E* **74** (2), 025301(R) (2006).

[4] T. A. Shaw, J.-L. Thiffeault, and C. R. Doering, 'Stirring up trouble: Multi-scale mixing measures for steady scalar sources,' *Physica D* **231** (2), 143–164 (2007).

[5] T. Okabe, B. Eckhardt, J.-L. Thiffeault, and C. R. Doering, 'Mixing effectiveness depends on the source–sink structure: Simulation results,' *Journal of Statistical Mechanics: Theory and Experiment* **2008** (7), P07018 (2008).

[6] L. Ó Náraigh and J.-L. Thiffeault, 'Bounds on the mixing enhancement for a stirred binary fluid,' *Physica D* **237** (21), 2673–2684 (2008).

[7] J.-L. Thiffeault and G. A. Pavliotis, 'Optimizing the source distribution in fluid mixing,' *Physica D* **237** (7), 918–929 (2008).

[8] S. Plasting and W. R. Young, 'A bound on scalar variance for the advection–diffusion equation,' *J. Fluid Mech.* **552**, 289–298 (2006).

[9] D. A. Birch, Y.-K. Tsang, and W. R. Young, 'Bounding biomass in the Fisher equation,' *Phys. Rev. E* **75**, 066304 (2007).

[10] S. R. Keating, P. R. Kramer, and K. S. Smith, 'Homogenization and mixing measures for a replenishing passive scalar field,' (2009), preprint.

[11] M. R. Turner, J. Thuburn, and A. D. Gilbert, 'The influence of periodic islands in the flow on a scalar tracer in the presence of a steady source,' *Phys. Fluids* **21**, 067103 (2009).

[12] E. Balkovsky and A. Fouxon, 'Universal long-time properties of Lagrangian statistics in the Batchelor regime and their application to the passive scalar problem,' *Phys. Rev. E* **60** (4), 4164–4174 (1999).

[13] E. Gouillart, O. Dauchot, J.-L. Thiffeault, and S. Roux, 'Open-flow mixing: Experimental evidence for strange eigenmodes,' *Phys. Fluids* **21** (2), 022603 (2009).

[14] E. Gouillart, O. Dauchot, and J.-L. Thiffeault, 'Measures of mixing quality in open flows with chaotic advection,' (2010), in preparation.

[15] P. V. Danckwerts, 'Continuous flow systems – distribution of residence times,' *Chem. Eng. Sci.* **2**, 1–13 (1953).

[16] H. M. Hulburt, 'Chemical processes in continuous-flow systems,' *Ind. Eng. Chem.* **36** (11), 1012–1017 (1944).

[17] J. R. A. Pearson, 'A note on the "Danckwerts" boundary conditions for continuous flow reactors,' *Chem. Eng. Sci.* **10**, 281–284 (1959).

[18] E. B. Nauman, 'Residence time distributions in systems governed by the dispersion equation,' *Chem. Eng. Sci.* **36** (6), 957–966 (1981).

[19] A. Hisaka and Y. Sugiyama, 'Notes on the inverse Gaussian distribution and choice of boundary conditions for the dispersion model in the analysis of local pharmacokinetics,' *J. Pharm. Sci.* **88** (12), 1362–1365 (1999).

[20] H. Aref, 'Stirring by chaotic advection,' *J. Fluid Mech.* **143**, 1–21 (1984).